



Regressor-free adaptive vibration control of constrained smart beams with axial stretching

Hayder F. N. Al-Shuka¹  · Ehab N. Abas²Received: 30 April 2020 / Accepted: 6 November 2020 / Published online: 4 December 2020
© Springer Nature Switzerland AG 2020

Abstract

This paper proposes an adaptive approximation control AAC technique (or so-called regressor-free adaptive control) for vibration regulation of constrained flexible smart beams with axial stretching. The key idea of the AAC is to control/regulate the target dynamic system while estimating the uncertainty using weighting and basis function terms with guaranteed stability based on Lyapunov theory. Accordingly, the dynamic equation of transverse vibration of the pinned–pinned smart beam is derived considering the effect of axial stretching. Due to the presence of a coupled tension–bending effect, a nonlinearly coupled cubic stiffness term appears in beam modelling making the dynamic system highly nonlinear. The resulted partial differential equation of the vibrating smart beam is discretized into definite N-mode shapes (definite degrees-of-freedom) using the Galerkin approach and a standard multi–input–multi–output ordinary differential equations system is established. Then two decoupled nonlinear control algorithms are designed based on the AAC for vibration attenuation of the nonlinear vibrating beam system. A pinned–pinned piezoelectrically-actuated/sensed flexible beam is simulated and the results show the validity of the proposed control architecture.

Keywords Smart structures · Adaptive approximation control · Regressor-free adaptive control · Nonlinear vibration

1 Introduction

Smart structures (or so-called adaptive or intelligent structures) have superior characteristics over traditional structures via structural health monitoring, damage detection, and damping out vibrations or even modification of their shapes [1]. They are provided with intelligent materials that can change their properties controllably if subjected to stimuli such as stress, strain or electric fields etc. Therefore, they can behave as actuators and sensors and can play important roles in the control of vibrating structures. Examples of smart materials are piezoelectric materials, shape-memory materials, electroactive polymers, etc. The current work is concerned with piezoelectric patches (sensor/actuators) that have the capability for vibration

suppression of slender structures. Flexible beam-like structures are of interested due to their wide applications in industry such as aerospace structures or flexible robotic manipulators etc. If a flexible structure is subjected to an excitation force, it vibrates frequently and a controller/regulator is required to attenuate or suppress the vibration motion. However, bonding piezo-patches to the surface of the vibrating system can stabilize the dynamic system and damp out the produced oscillations. The vibrating beam-like structures have infinite degrees of freedom and hence a partial differential equation PDE is obtained. However, the difficulty of the solution of the resulted PDE depends on the imposed assumptions for the target problem. Accordingly, three well-known theories are available for modelling of beam structures: (1) Euler–Bernoulli beam

✉ Hayder F. N. Al-Shuka, hayder.al-shuka@rwth-aachen.de; hayder.alshuka@gmail.com | ¹Department of Aeronautical Engineering, University of Baghdad, Baghdad, Iraq. ²Ministry of Higher Education and Scientific Research, Studies and Planning and Follow Up Directorate, Baghdad, Iraq.



theory in which the rotational inertia and shear deformation are neglected, (2) Rayleigh theory that considers the rotational inertia only, and (3) Timoshenko theory in which both rotational inertia and shear deformations are considered [2]. The resulted PDE of the vibrating structure is transformed into N-ordinary differential equations ODEs, with N denoting the number of mode shapes of the target structure, using the Galerkin approach. The idea is to separate the displacement and time spaces and hence N-ODEs are obtained. Consequently, this work is focused on modelling and control of constrained Euler–Bernoulli beam with axial stretching. The axial stretching results from deflection of the beam rather than the application of pure axial loading. Accordingly, the resulted ODEs are no longer linear and nonlinear control approaches are required. For modelling of nonlinear vibration of beam-like structures, the reader is referred to [3–5].

Careful design of vibration control for flexible structures is demanded due to the presence of multiple resonances in the frequency response of the dynamic system. Besides, bonding the piezo-actuators to the vibrating beam may excite the strong resonances. Therefore, the design of feedback control is not trivially selected and the stability of the control architecture should be ensured [6]. The possible control methods to deal with nonlinear vibrations are (see Chap. 3 of [6]) linear velocity control (integral acceleration feedback control), (2) PID-type control, (3) Feedback linearization, (4) adaptive control, and (5) robust control [6–9]. In velocity control, the input control is selected as integral of the system acceleration and hence a damping term is added to the dynamic equation of the smart beam that reduces the amplitudes of the resonances. The well-known PID-type control is extensively used in stabilization of second-order dynamic systems. Under specifically tuned gains, the closed-loop dynamics can be reduced to the first-order system with acceptable tracking or regulation. However, these gains are limited by stability conditions and hence PID control works well within the low-frequency region below the cut-off frequency. Therefore, using a feedforward term with the feedback PID can improve the system stability and makes the system work with infinite control bandwidth [10]. However, if unmodeled dynamics exist adaptive or sliding mode control approaches are good choices. Sliding mode control selects a sliding surface in terms of position/velocity errors and a signum function plays an important role in control architecture. Due to discontinuous behaviour of signum function, alternative continuous functions are used such as tanh function but with bounded error due to approximation. Higher-order sliding mode control is suggested to solve the discontinuous problem but the complexity of computations may result, see [11] for more details. On the other hand, adaptive control associated with Slotine-Li

approach is a powerful control law for the control of nonlinear rigid/flexible body systems [12]. It integrates both the feedforward and feedback terms under uncertainty. The key idea of adaptive control is to linearly parameterize of the dynamic equation such that the left-hand side of the equation of motion is decomposed in terms of regressor matrix that is a function of state variables and uncertain constant parameters vector. Regressor-based adaptive control deals with uncertain constant parameters and a robust sliding term or robust learning algorithms are required to compensate for modelling error and disturbances [12]. On the other hand, adaptive approximation control is a powerful tool to control the nonlinear dynamic system with time-varying disturbances. The uncertainty is approximated by weighting and basis function matrices and then the weighting matrices are updated based on Lyapunov theory. For more information on this topic, the reader is referred to [13–15].

Accordingly, the current work is focused on the design of the function approximation technique FAT-based adaptive control for the flexible smart beam with axial stretching. The uncertain terms/coefficients are approximated using weighting and orthogonal basis function vectors/matrices. The strength of the AAC is that it is a modular decentralized control law that can deal with N-mode shapes individually. On the other hand, the nonlinearly coupled cubic stiffness term is easily compensated using the proposed control architecture. A pinned–pinned smart beam is simulated and the results show the validity of the proposed control architecture.

The rest of the paper is organized as follows. The dynamic modelling of the vibrating smart beam and the control architecture is introduced in Sect. 2. Whereas the results are presented and discussed in Sect. 3. Section 4 concludes.

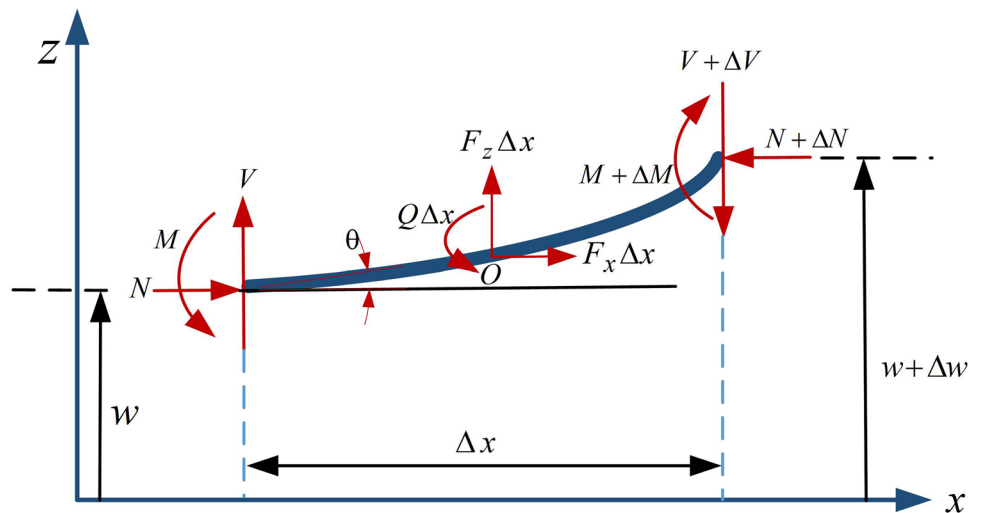
2 Methodology

2.1 Dynamic modelling

Consider an element of a constrained beam (e.g., a pinned–pinned beam) vibrating in the x – z plane with internal forces and moments and their increments acting at its ends, see Fig. 1. The beam element is subjected to external (applied) force and moment functions F_x, F_z, Q respectively applied at point O (centre of the beam element). These forces/moments can include inertial terms and applied piezo-moments. Before going deeply into the derivation of the equation of beam, the following assumptions are proposed:

Assumption 1 The effect of axial stretching is included.

Fig.1 The free-body diagram for an element of a vibrating beam



Assumption 2 The rotational inertial terms are neglected.

Assumption 3 The dynamics of piezo-patches are neglected.

Assumption 4 The modal amplitudes of the vibrating beam are measurable. This includes sufficient transducers (e.g. piezo-sensors) are available.

Most details of beam modelling are cited from [6, 16]. Applying Newton–Euler formulation on the beam element leads to the following partial differential equation PDE of transverse vibration deflection w under different dynamic loadings:

$$\frac{\partial^2 M}{\partial x^2} = F_x + T \frac{\partial^2 w}{\partial x^2} - \frac{\partial Q}{\partial x} \tag{1}$$

where M refers to the moment and T is the tension force acting along the target beam due to vibration of the constrained beam that has immovable supports. The tensile force T can be computed as

$$T = \frac{E_b A_b}{2l} \int_0^l \left(\frac{\partial w}{\partial x} \right)^2 dx \tag{2a}$$

where E_b , A_b and l_b are the Young’s modulus, cross-sectional area and the span of the beam respectively. Whereas, the force/moment terms of Eq. (1) can be evaluated as

$$M = E_b I_b \frac{\partial \theta}{\partial s} = E_b I_b \frac{\partial^2 w}{\partial x^2} \tag{2b}$$

where θ is the slope of deflected beam and s is the length of the beam. Equation (2b) has been obtained according

to Assumption 1 such that the following expressions hold: $\Delta s \approx \Delta x$, $\partial s / \partial x \approx 1$, $\theta \approx \sin \theta = \Delta w / \Delta x$ or $\theta = \partial w / \partial x$. In addition,

$$F_x = f(x, t) - \rho_b A_b \frac{\partial^2 w}{\partial t^2} \tag{2c}$$

where $f(x, t)$ is the force per unit length distributed along the span of the beam and ρ_b is the density of the beam. Whereas, the applied moment can be calculated as

$$Q = \frac{\partial M_p}{\partial x}, M_p = D v_a(t) \frac{\partial^2}{\partial x^2} [H(x - x_1) - H(x - x_2)] \tag{2d}$$

where M_p is the applied piezo-moment that is necessary to suppress the beam vibration, D is a constant that depends on physical parameters of the regular beam and the piezo-actuator, see [17] for more details on the evaluation of this constant, and $H(\cdot)$ is a Heaviside step function. Substituting Eqs. (2a–d) into Eq. (1) to get the following partial differential equation:

$$E_b I_b \frac{\partial^4 w}{\partial x^4} - \frac{E_b A_b}{2l_b} \int_0^l \left(\frac{\partial w}{\partial x} \right)^2 dx \left(\frac{\partial^2 w}{\partial x^2} \right) + \rho_b A_b \frac{\partial^2 w}{\partial t^2} = f(x, t) - \frac{\partial^2 M_p}{\partial x^2} \tag{3}$$

It should be noted that Eq. (3) is a nonlinear PDE due to the second term that is associated with axial stretching. Now it is time to transform infinite degrees-of-freedom DoF-PDE described in Eq. (3) into N -ODEs using Galerkin modal decomposition with N being referred to the number of mode shapes. Accordingly, using the principle of separation of variables, the transverse deflection of the beam can be approximated as

$$w(x, t) = \sum_{i=1}^N \varphi_i(x)q_i(t) \tag{4}$$

$$\left(\frac{\rho_b A_b l_b}{2}\right) \ddot{q}_n + \left(\frac{E_b l_b \lambda_n^4}{2}\right) q_n + \left(\frac{E_b A_b \pi^4 n^2}{8 l_b^3}\right)$$

where $\varphi_i(x)$ is the i th mode shape and $q_i(t)$ is the corresponding time-dependent generalized coordinate (amplitude).

Substituting Eq. (4) into Eq. (3) to get

$$\sum_{k=1}^N k^2 q_k^2 q_n = g_n(x, t) - \mu_n v_a(t), \quad n = 1, 2, 3, \dots, N \tag{7a}$$

$$\sum_{i=1}^N \left[E_b l_b \frac{d^4 \varphi_i}{dx^4} q_i - \frac{E_b A_b}{2 l_b} \sum_{j=1}^N \sum_{k=1}^N \int_0^{l_b} \left(\frac{d\varphi_j}{dx} q_j\right) \left(\frac{d\varphi_k}{dx} q_k\right) dx \left(\frac{d^2 \varphi_i}{dx^2}\right) q_i + \rho_b A_b \varphi_i \ddot{q}_i \right] \tag{5}$$

$$= f(x, t) - D v_a \frac{\partial^2}{\partial x^2} [H(x - x_1) - H(x - x_2)]$$

Below we will consider the case of modelling and modal control of pinned–pinned beams with the following associated mathematical relations.

The i -mode shape is:

$$\varphi_i = \sin(i\pi \frac{x}{l_b}) \tag{6a}$$

The natural linearized frequency is:

$$\omega_i = \lambda_i^2 \sqrt{\frac{E_b l_b}{\rho_b A_b}}, \lambda_i = \frac{i\pi}{l_b} \tag{6b}$$

The orthogonality conditions are:

$$\int_0^{l_b} \varphi_i \varphi_j dx = l_b / 2, \int_0^{l_b} \varphi_i'''' \varphi_j dx = \begin{cases} (l_b/2) \lambda_i^4, & i = j \\ 0, & i \neq j \end{cases} \tag{6c}$$

In addition, according to Eq. (6a), the following integral and differentiation are obtained:

$$\int_0^{l_b} \left(\frac{d\varphi_i}{dx}\right) \left(\frac{d\varphi_j}{dx}\right) dx = \begin{cases} j^2 \pi^2 / 2 l_b, & i = j \\ 0, & i \neq j \end{cases} \tag{6d}$$

$$\frac{d^2 \varphi_i}{dx^2} = -\lambda_i^2 \varphi_i \tag{6e}$$

Multiplication of Eq. (5) by an arbitrary mode shape, φ_n , and exploiting the above mathematical formulae, Eq. (6a–e), we can get the following ODEs for an n -mode shape:

where $\mu_n = D(\varphi_n'(x_2) - \varphi_n'(x_1))$, $g_n(x, t) = \int_0^{l_b} f(x, t) \varphi_n(x) dx$.

It should be noted that the first two terms on the left-hand side of Eq. (7a) are decoupled while the last third term is nonlinearly coupled. For example, considering $n = 1$ leads to an equation that is similar to Duffing oscillator with a cubic stiffness term [6]. On the other side, Eq. (7a) includes one piezo-actuator placed on the surface of the target beam. In effect, N_a actuators can be placed on the beam for vibration suppression purpose. Thus, Eq. (7a) can be modified to get

$$\left(\frac{\rho_b A_b l_b}{2}\right) \ddot{q}_n + \left(\frac{E_b l_b \lambda_n^4}{2}\right) q_n + \left(\frac{E_b A_b \pi^4 n^2}{8 l_b^3}\right) \sum_{k=1}^N k^2 q_k^2 q_n = g_n(x, t) - \sum_{j=1}^{N_a} \mu_{nj} v_{aj}(t), \quad n = 1, 2, 3, \dots, N \tag{7b}$$

with

$$\mu_{nj} = D(\varphi_n'(x_{2j}) - \varphi_n'(x_{1j}))$$

Remark 1 Equation (7b) does not consider the model damping while the model must have some damping. Despite there are several ways to deal with damping effect, the easiest way is to add a viscous damping term for each mode after Galerkin approach has been performed [6]. However, this method has limitations in applications where the damping is non-viscous. For more details on this topic, the reader is referred to [18].

According to Remark 1 with further manipulation, we get

$$m_n \ddot{q}_n + b_n \dot{q}_n + k_n q_n + \eta_n - g_n(x, t) = u_n, \quad n = 1, 2, 3, \dots, N \tag{7c}$$

$$v_{sj} = \sum_{k=1}^N \alpha_{jk} q_k(t) = [\alpha_{j1} \dots \alpha_{jN}] \begin{bmatrix} q_1 \\ \vdots \\ q_N \end{bmatrix}, \quad j = 1, 2, 3, \dots, N_s \tag{9}$$

with

$$m_n = \left(\frac{\rho_b A_b l_b}{2} \right), b_n = (2\zeta_n w_n) m_n, -1 \leq \zeta_n \leq 1, k_n = \frac{E_b l_b \lambda_n^4}{2}, w_n^2 = k_n / m_n,$$

$$\eta_n = \left(\frac{E_b A_b \pi^4 n^2}{8l_b^3} \right) \sum_{k=1}^N k^2 q_k^2 q_n, \quad u_n = -\mu_n v_a(t)$$

Equation (7c) can be represented in a matrix form as follows:

$$M\ddot{\mathbf{q}} + B\dot{\mathbf{q}} + K\mathbf{q} + \boldsymbol{\eta} + \mathbf{g} = \mathbf{u} \tag{8}$$

where $\alpha_{(j)}$ is a constant that depends on the location of piezoelectric sensors and N_s is the number of piezoelectric sensors that is equal to N_a in case of collocated patches [17]. In matrix/vector representation, Eq. (9) can be rewritten as

$$\mathbf{q} = \begin{bmatrix} q_1 \\ \vdots \\ q_N \end{bmatrix} \in R^N, \mathbf{M} = \begin{bmatrix} m_1 & \dots & 0 \\ \vdots & \ddots & \vdots \\ 0 & \dots & m_N \end{bmatrix} \in R^{N \times N}, \mathbf{B} = \begin{bmatrix} b_1 & \dots & 0 \\ \vdots & \ddots & \vdots \\ 0 & \dots & b_N \end{bmatrix}, \mathbf{K} = \begin{bmatrix} k_1 & \dots & 0 \\ \vdots & \ddots & \vdots \\ 0 & \dots & k_N \end{bmatrix} \in R^{N \times N},$$

$$\boldsymbol{\eta} = \begin{bmatrix} \eta_1 \\ \vdots \\ \eta_N \end{bmatrix} \in R^N, \mathbf{g} = \begin{bmatrix} -g_1 \\ \vdots \\ -g_N \end{bmatrix} \in R^N, \mathbf{u} = \begin{bmatrix} u_1 \\ \vdots \\ u_N \end{bmatrix} = - \begin{bmatrix} \mu_{11} & \dots & \mu_{1N_a} \\ \vdots & \ddots & \vdots \\ \mu_{N1} & \dots & \mu_{NN_a} \end{bmatrix} \begin{bmatrix} v_{a1} \\ \vdots \\ v_{aN_a} \end{bmatrix} \in R^N$$

Remark 2

1. Due to the nonlinear elastic restoring force vector $\boldsymbol{\eta}$, Eq. (8) has nonlinear behaviour and requires advanced nonlinear control methods to regulate the vibration motion, this is well treated in the next section.
2. The pseudo-inverse matrix plays an important role in evaluation of actuator voltages if $N \neq N_a$, see [7] for more details.
3. Fortunately, there is a linear relationship between the sensor voltages v_s and the modal amplitudes \mathbf{q} and hence most literature used v_s as state variables instead of \mathbf{q} . Thus,

$$\mathbf{v} = \boldsymbol{\alpha} \mathbf{q}, \quad \boldsymbol{\alpha} = \begin{pmatrix} \alpha_{11} & \dots & \alpha_{1N} \\ \vdots & \ddots & \vdots \\ \alpha_{N_s 1} & \dots & \alpha_{N_s N} \end{pmatrix} \in R^{N_s \times N} \tag{10}$$

Therefore, substituting Eq. (10) into Eq. (8) results in

$$\boldsymbol{\alpha}^+ M \ddot{\mathbf{v}}_s + \boldsymbol{\alpha}^+ B \dot{\mathbf{v}}_s + \boldsymbol{\alpha}^+ K \mathbf{v}_s + \mathbf{g} + \boldsymbol{\eta} = \mathbf{u} \tag{11a}$$

or

$$\bar{M} \ddot{\mathbf{v}}_s + \bar{B} \dot{\mathbf{v}}_s + \bar{K} \mathbf{v}_s + \mathbf{g} + \boldsymbol{\eta} = \mathbf{u} \tag{11b}$$

with

$$\bar{\mathbf{M}} = \alpha^+ \mathbf{M}, \bar{\mathbf{B}} = \alpha^+ \mathbf{B}, \bar{\mathbf{K}} = \alpha^+ \mathbf{K}$$

where $\alpha^+ \in R^{N \times N}$, is the Moore–Penrose inverse of sensor gain matrix (α).

2.2 The control architecture

The proposed controller aims at suppressing the vibration motion of the target beam. The input control is provided by the piezo-actuator while the beam deflection is sensed indirectly via the sensor voltages (or equivalently modal amplitudes). Consequently, this section is focused on regressor-free adaptive control. The key idea is to approximate the uncertain coefficients/terms of the equation of motion by using linear combinations of basis functions such as fuzzy, neural, or orthogonal basis function approximators, etc. Then the unknown coefficients of the basis functions are updated based on Lyapunov theory. Now let us represent the dynamic coefficients/terms of Eq. (8) in terms of the weighting coefficient and orthogonal basis function vectors as follows.

$$\begin{aligned} \mathbf{M} &= \begin{bmatrix} m_1 & \dots & 0 \\ \vdots & \ddots & \vdots \\ 0 & \dots & m_N \end{bmatrix} = \begin{bmatrix} \mathbf{c}_{m_1}^T \boldsymbol{\Psi}_{m_1} & \dots & 0 \\ \vdots & \ddots & \vdots \\ 0 & \dots & \mathbf{c}_{m_N}^T \boldsymbol{\Psi}_{m_N} \end{bmatrix} + \boldsymbol{\varepsilon}_M = \begin{bmatrix} \mathbf{c}_{m_1}^T & \dots & \mathbf{0}^T \\ \vdots & \ddots & \vdots \\ \mathbf{0}^T & \dots & \mathbf{c}_{m_N}^T \end{bmatrix} \begin{bmatrix} \boldsymbol{\Psi}_{m_1} & \dots & \mathbf{0} \\ \vdots & \ddots & \vdots \\ \mathbf{0} & \dots & \boldsymbol{\Psi}_{m_N} \end{bmatrix} + \boldsymbol{\varepsilon}_M \\ &= \mathbf{C}_M^T \boldsymbol{\Psi}_M + \boldsymbol{\varepsilon}_M \\ \mathbf{B} &= \begin{bmatrix} b_1 & \dots & 0 \\ \vdots & \ddots & \vdots \\ 0 & \dots & b_N \end{bmatrix} = \begin{bmatrix} \mathbf{c}_{b_1}^T \boldsymbol{\Psi}_{b_1} & \dots & 0 \\ \vdots & \ddots & \vdots \\ 0 & \dots & \mathbf{c}_{b_N}^T \boldsymbol{\Psi}_{b_N} \end{bmatrix} + \boldsymbol{\varepsilon}_B = \begin{bmatrix} \mathbf{c}_{b_1}^T & \dots & \mathbf{0}^T \\ \vdots & \ddots & \vdots \\ \mathbf{0}^T & \dots & \mathbf{c}_{b_N}^T \end{bmatrix} \begin{bmatrix} \boldsymbol{\Psi}_{b_1} & \dots & \mathbf{0} \\ \vdots & \ddots & \vdots \\ \mathbf{0} & \dots & \boldsymbol{\Psi}_{b_N} \end{bmatrix} + \boldsymbol{\varepsilon}_B \\ &= \mathbf{C}_B^T \boldsymbol{\Psi}_B + \boldsymbol{\varepsilon}_B \\ \mathbf{K} \mathbf{q} &= \begin{bmatrix} k_1 q_1 \\ \vdots \\ k_N q_N \end{bmatrix} = \begin{bmatrix} \mathbf{c}_{K_1}^T \boldsymbol{\Psi}_{K_1} \\ \vdots \\ \mathbf{c}_{K_N}^T \boldsymbol{\Psi}_{K_N} \end{bmatrix} + \boldsymbol{\varepsilon}_K = \begin{bmatrix} \mathbf{c}_{K_1}^T & \dots & \mathbf{0}^T \\ \vdots & \ddots & \vdots \\ \mathbf{0}^T & \dots & \mathbf{c}_{K_N}^T \end{bmatrix} \begin{bmatrix} \boldsymbol{\Psi}_{K_1} \\ \vdots \\ \boldsymbol{\Psi}_{K_N} \end{bmatrix} = \mathbf{C}_K^T \bar{\boldsymbol{\Psi}}_K + \boldsymbol{\varepsilon}_K \\ \boldsymbol{\eta} &= \begin{bmatrix} \eta_1 \\ \vdots \\ \eta_N \end{bmatrix} = \begin{bmatrix} \mathbf{c}_{\eta_1}^T \boldsymbol{\Psi}_{\eta_1} \\ \vdots \\ \mathbf{c}_{\eta_N}^T \boldsymbol{\Psi}_{\eta_N} \end{bmatrix} + \boldsymbol{\varepsilon}_\eta = \begin{bmatrix} \mathbf{c}_{\eta_1}^T & \dots & \mathbf{0}^T \\ \vdots & \ddots & \vdots \\ \mathbf{0}^T & \dots & \mathbf{c}_{\eta_N}^T \end{bmatrix} \begin{bmatrix} \boldsymbol{\Psi}_{\eta_1} \\ \vdots \\ \boldsymbol{\Psi}_{\eta_N} \end{bmatrix} = \mathbf{C}_\eta^T \bar{\boldsymbol{\Psi}}_\eta + \boldsymbol{\varepsilon}_\eta \\ \mathbf{g} &= \begin{bmatrix} -g_1 \\ \vdots \\ -g_N \end{bmatrix} = \begin{bmatrix} \mathbf{c}_{g_1}^T \boldsymbol{\Psi}_{g_1} \\ \vdots \\ \mathbf{c}_{g_N}^T \boldsymbol{\Psi}_{g_N} \end{bmatrix} + \boldsymbol{\varepsilon}_g = \begin{bmatrix} \mathbf{c}_{g_1}^T & \dots & \mathbf{0}^T \\ \vdots & \ddots & \vdots \\ \mathbf{0}^T & \dots & \mathbf{c}_{g_N}^T \end{bmatrix} \begin{bmatrix} \boldsymbol{\Psi}_{g_1} \\ \vdots \\ \boldsymbol{\Psi}_{g_N} \end{bmatrix} = \mathbf{C}_g^T \bar{\boldsymbol{\Psi}}_g + \boldsymbol{\varepsilon}_g \end{aligned} \tag{12}$$

where $\mathbf{C}_{(\cdot)} \in R^{N \times N}$ is the weighting coefficient matrix, $\boldsymbol{\Psi}_{(\cdot)} \in R^{N \times N}$ is the orthogonal basis matrix associated with the mass, $\bar{\boldsymbol{\Psi}}_{(\cdot)} \in R^{N \times 1}$ is an orthogonal basis vector, and $\boldsymbol{\varepsilon}_{(\cdot)} \in R^N$ is the approximation error vector.

Thus, the equation of vibration motion, Eq. (8), can be reformulated exploiting Eq. (12) to get

$$\mathbf{C}_M^T \boldsymbol{\Psi}_M \ddot{\mathbf{q}} + \mathbf{C}_B^T \boldsymbol{\Psi}_B \dot{\mathbf{q}} + \mathbf{C}_K^T \bar{\boldsymbol{\Psi}}_K + \mathbf{C}_\eta^T \bar{\boldsymbol{\Psi}}_\eta + \mathbf{C}_g^T \bar{\boldsymbol{\Psi}}_g + \sum \boldsymbol{\varepsilon} = \mathbf{u} \tag{13}$$

where $\boldsymbol{\varepsilon}$ is the accumulated approximation error. For simplicity, Eq. (13) can be further approximated as follows:

$$\mathbf{C}_M^T \boldsymbol{\Psi}_M \ddot{\mathbf{q}} + \mathbf{C}_B^T \boldsymbol{\Psi}_B \dot{\mathbf{q}} + \mathbf{C}_n^T \bar{\boldsymbol{\Psi}}_n + \sum \boldsymbol{\varepsilon} = \mathbf{u} \tag{14}$$

with

$$\mathbf{C}_n^T \bar{\boldsymbol{\Psi}}_n = \mathbf{C}_\eta^T \bar{\boldsymbol{\Psi}}_\eta + \mathbf{C}_g^T \bar{\boldsymbol{\Psi}}_g$$

The intuitive control law that is suitable for Eq. (14) can be designed as [14, 15]

$$\mathbf{u} = \hat{\mathbf{C}}_M^T \boldsymbol{\Psi}_M \ddot{\mathbf{q}}_r + \hat{\mathbf{C}}_B^T \boldsymbol{\Psi}_B \dot{\mathbf{q}}_r + \hat{\mathbf{C}}_n^T \bar{\boldsymbol{\Psi}}_n + \mathbf{K}_d \mathbf{s} \tag{15a}$$

with the following update laws for the unknown coefficient matrices

$$\begin{aligned} \dot{\hat{\mathbf{C}}}_M &= \mathbf{Q}_M^{-1} \boldsymbol{\Psi}_M \ddot{\mathbf{q}}_r \mathbf{s}^T \\ \dot{\hat{\mathbf{C}}}_B &= \mathbf{Q}_B^{-1} \boldsymbol{\Psi}_B \dot{\mathbf{q}}_r \mathbf{s}^T \\ \dot{\hat{\mathbf{C}}}_n &= \mathbf{Q}_n^{-1} \bar{\boldsymbol{\Psi}}_n \mathbf{s}^T \end{aligned} \tag{15b}$$

where the symbol $(\hat{\cdot})$ refers to the estimation, $\mathbf{K}_d \in R^{N \times N}$ is a high gain positive diagonal matrix, and

$$\dot{\mathbf{q}}_r = \dot{\mathbf{q}}_d + \boldsymbol{\Lambda}(\mathbf{q}_d - \mathbf{q}), \mathbf{s} = \dot{\mathbf{q}}_r - \dot{\mathbf{q}} = \dot{\mathbf{e}} + \boldsymbol{\Lambda} \mathbf{e}$$

where $\dot{\mathbf{q}}_r \in R^N$ is the required velocity vector and it is equal to the desired velocity trajectory $\dot{\mathbf{q}}_d \in R^N$ plus the position error. Whereas, $\mathbf{s} \in R^N$ is an auxiliary error vector that consists of proportional-derivative PD control terms.

Subtracting Eq. (14) from Eq. (15a) leads to the following closed-loop dynamics:

$$\mathbf{M}\dot{\mathbf{s}} + \mathbf{B}\mathbf{s} + \mathbf{K}_d\mathbf{s} = \tilde{\mathbf{C}}_M^T \Psi_M \ddot{\mathbf{q}}_r + \tilde{\mathbf{C}}_B^T \Psi_B \dot{\mathbf{q}}_r + \tilde{\mathbf{C}}_n^T \bar{\Psi}_n + \boldsymbol{\varepsilon}, \quad \boldsymbol{\varepsilon} = \sum (\boldsymbol{\varepsilon}_M + \boldsymbol{\varepsilon}_B + \boldsymbol{\varepsilon}_n) \tag{17}$$

where $\boldsymbol{\varepsilon}^T \boldsymbol{\Omega} \boldsymbol{\varepsilon} \leq \bar{\varepsilon}$, with $\boldsymbol{\Omega} \in R^{N \times N}$ being a positive definite matrix.

Lemma 1 *The dynamic modelling of the smart beam represented by Eq. (8) with the control law, update laws described in Eq. (15) and the closed-loop dynamics given in Eq. (17) is stable in the sense of Lyapunov theory provided that $\mathbf{K}_d + \mathbf{B} > \boldsymbol{\Omega}^{-1}$.*

Proof Let us consider the following Lyapunov function candidate along Eq. (17)

$$V = \frac{1}{2} \mathbf{s}^T \mathbf{M} \mathbf{s} + \frac{1}{2} \text{tr}(\tilde{\mathbf{C}}_M^T \mathbf{Q}_M \tilde{\mathbf{C}}_M + \tilde{\mathbf{C}}_B^T \mathbf{Q}_B \tilde{\mathbf{C}}_B + \tilde{\mathbf{C}}_n^T \mathbf{Q}_n \tilde{\mathbf{C}}_n) \tag{18}$$

Differentiating Eq. (18) and substituting Eq. (17) to get

$$\dot{V} = \mathbf{s}^T (-\mathbf{B}\mathbf{s} - \mathbf{K}_d\mathbf{s} + \tilde{\mathbf{C}}_M^T \Psi_M \ddot{\mathbf{q}}_r + \tilde{\mathbf{C}}_B^T \Psi_B \dot{\mathbf{q}}_r + \tilde{\mathbf{C}}_n^T \bar{\Psi}_n + \boldsymbol{\varepsilon}) + \frac{1}{2} \mathbf{s}^T \dot{\mathbf{M}} \mathbf{s} - \text{tr}(\tilde{\mathbf{C}}_M^T \mathbf{Q}_M \dot{\tilde{\mathbf{C}}}_M + \tilde{\mathbf{C}}_B^T \mathbf{Q}_B \dot{\tilde{\mathbf{C}}}_B + \tilde{\mathbf{C}}_n^T \mathbf{Q}_n \dot{\tilde{\mathbf{C}}}_n) \tag{19}$$

But $\dot{\mathbf{M}} = \mathbf{0}$, then we can get

$$\dot{V} = -\mathbf{s}^T \mathbf{B} \mathbf{s} - \mathbf{s}^T \mathbf{K}_d \mathbf{s} - \text{tr}(\tilde{\mathbf{C}}_M^T (\Psi_M \ddot{\mathbf{q}}_r \mathbf{s}^T - \mathbf{Q}_M \dot{\tilde{\mathbf{C}}}_M)) - \text{tr}(\tilde{\mathbf{C}}_B^T (\Psi_B \dot{\mathbf{q}}_r \mathbf{s}^T - \mathbf{Q}_B \dot{\tilde{\mathbf{C}}}_B)) - \text{tr}(\tilde{\mathbf{C}}_n^T (\bar{\Psi}_n \mathbf{s}^T - \mathbf{Q}_n \dot{\tilde{\mathbf{C}}}_n)) + \mathbf{s}^T \boldsymbol{\varepsilon} \tag{20}$$

Substituting Eq. (15b) into above equation to obtain

$$\dot{V} = -\mathbf{s}^T \mathbf{B} \mathbf{s} - \mathbf{s}^T \mathbf{K}_d \mathbf{s} + \mathbf{s}^T \boldsymbol{\varepsilon} \tag{21}$$

Using the following inequality [19]

$$\mathbf{s}^T \boldsymbol{\varepsilon} \leq \mathbf{s}^T \boldsymbol{\Omega}^{-1} \mathbf{s} + \boldsymbol{\varepsilon}^T \boldsymbol{\Omega} \boldsymbol{\varepsilon} \leq \mathbf{s}^T \boldsymbol{\Omega}^{-1} \mathbf{s} + \bar{\varepsilon} \tag{22}$$

Thus, Eq. (21) becomes

$$\dot{V} \leq -\mathbf{s}^T (\mathbf{K}_d + \mathbf{B} - \boldsymbol{\Omega}^{-1}) \mathbf{s} + \bar{\varepsilon} \tag{23}$$

where $\bar{\varepsilon}$ is the upper bound of $\boldsymbol{\varepsilon}$. To ensure stability, it is necessary to have $\mathbf{K}_d + \mathbf{B} > \boldsymbol{\Omega}^{-1}$, then the tracking error is bounded and $\|\mathbf{s}\|^2$ converges to $\bar{\varepsilon}$.

Remark 3 The control law described in Eq. (15) is fully decentralized due to the diagonal matrix of the weighting matrix and hence it is a powerful tool to suppress vibration of multi-mode shapes for the vibrating beam.

Remark 4 In effect, the total terms on left-hand side of Eq. (8) can be approximated in terms of the weighting

Fig. 2 a A simply supported beam with two piezo-patches and concentrated excitation force located at the middle of the beam. **b** The time-history profile of the excitation force

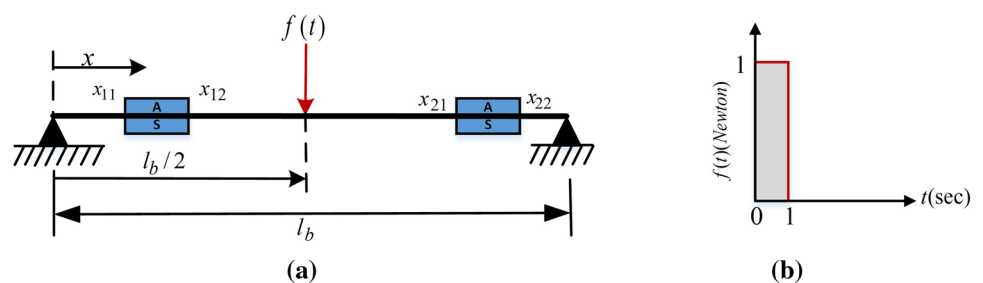


Table 1 Numerical values used in simulation experiments

Beam	$\rho_b = 8030 \text{ kg/m}^3, l_b = 0.3 \text{ m}, E_b = 193 \times 10^9 \text{ Pa}, A_b = 0.03 \times 0.0005 \text{ m}$, where the subscript b refers to the regular beam. The damping constants for the first two modes are selected as $b_1 = 0.0068 \text{ Ns/m}, b_2 = 0.0280 \text{ Ns/m}^{**}$
Piezo-materials	$l_p = 0.075 \text{ m}, A_p = 0.025 \times 0.00035 \text{ m}, E_p = 68 \times 10^9 \text{ Pa}$, where the subscript p refers to the piezoelectric materials. $x_{11} = 0.0525 \text{ m}, x_{12} = 0.1275 \text{ m}, x_{21} = 0.1725 \text{ m}, x_{22} = 0.2475 \text{ m}$. For more details on evaluation of D and $\alpha_{(j)}$, see [17]
Feedback gains	$\Lambda = 20I_2, \mathbf{Q}_M^{-1} = 0.01I_{22}, \mathbf{Q}_n^{-1} = 75I_{22}, \mathbf{K}_d = 300I_2$ where I_n is an $n \times n$ identity matrix

**The damping constants are selected such that the vibrating smart beam is lightly damped

coefficient matrix and orthogonal basis vector and hence the control law can be designed as:

$$\mathbf{u} = \mathbf{K}_d \mathbf{s} + \hat{\mathbf{C}}_c^T \bar{\boldsymbol{\psi}}_c \quad (24a)$$

with the following updating laws:

$$\dot{\hat{\mathbf{C}}}_c = \mathbf{Q}_c^{-1} \bar{\boldsymbol{\psi}}_c \mathbf{s}^T \quad (24b)$$

where as the close-loop dynamics can be expressed as

$$\mathbf{M} \dot{\mathbf{s}} + \mathbf{K}_d \mathbf{s} = \tilde{\mathbf{C}}_c^T \bar{\boldsymbol{\psi}}_c + \boldsymbol{\delta} \quad (25)$$

where $\boldsymbol{\delta}$ is a bounded modelling error, $\boldsymbol{\delta}^T \bar{\boldsymbol{\Omega}} \boldsymbol{\delta} \leq \bar{\epsilon}$, with $\bar{\boldsymbol{\Omega}} \in R^{N \times N}$ being a positive definite matrix. The proof of stability is similar to Lemma 1.

3 Simulation results and discussions

Consider a flexible pinned–pinned beam with two piezo-patches located at suitable locations as depicted in Fig. 2. The physical parameters and feedback gains used in simulations are introduced in Table 1. An impulse force of value 1 N during 1 s is applied at a location $(l_b/2)$ to excite the vibration the beam. Since the dominant modes locate at the low-frequency region of the frequency response, the first two mode shapes are considered in our simulation experiments. Before going into the application of control architecture, let us recall Eq. (7c) but with $g_n(x, t) = 0$:

$$m_n \ddot{q}_n + b_n \dot{q}_n + k_n q_n + \eta_n = u_n, \quad n = 1, 2, 3, \dots, N \quad (26)$$

with

Fig. 3 Amplitude response with and without control

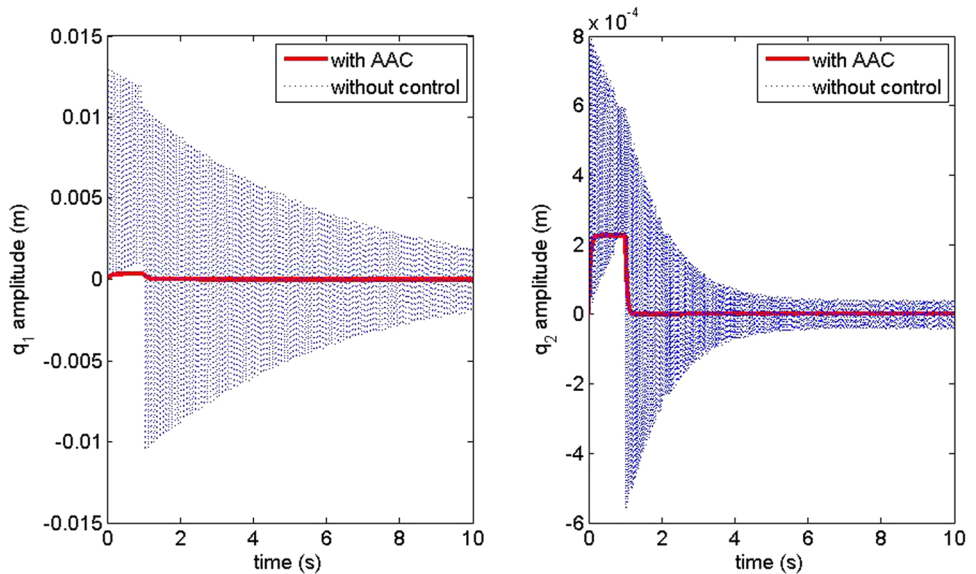


Fig. 4 Response of sensor voltage with and without control

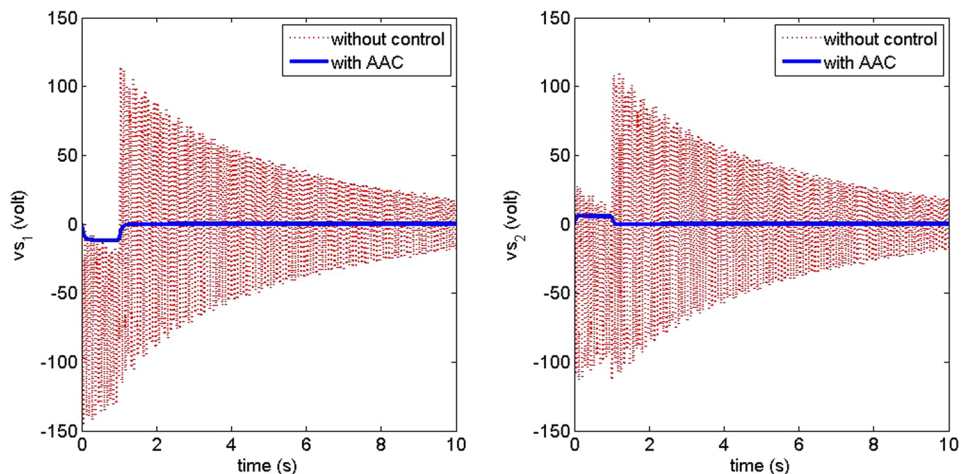
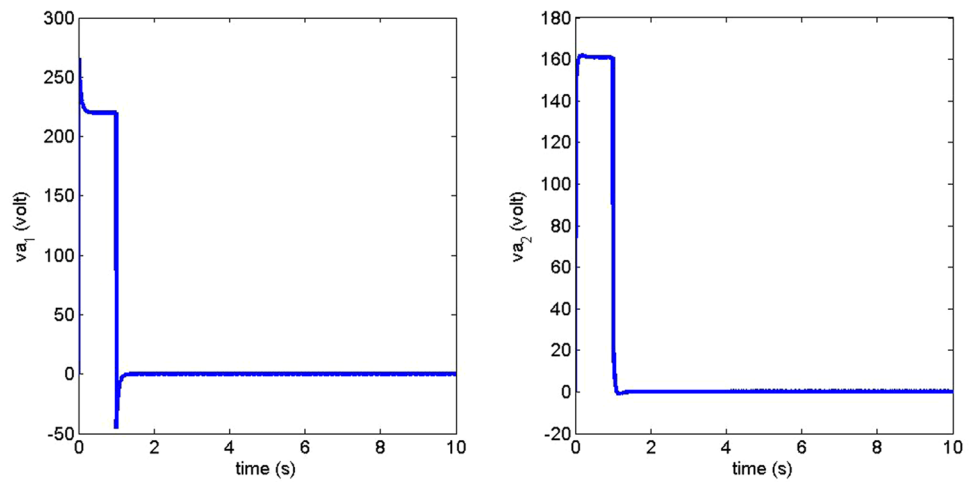


Fig. 5 Input control piezo-voltages



$$m_n = \left(\frac{\rho_b A_b l_b}{2} \right), b_n = (2\zeta_n w_n) m_n, -1 \leq \zeta_n \leq 1, k_n = \frac{E_b I_b \lambda_n^4}{2}, w_n^2 = k_n / m_n,$$

$$\eta_n = \left(\frac{E_b A_b \pi^4 n^2}{8 l_b^3} \right) \sum_{k=1}^N k^2 q_k^2 q_n, u_n = -\mu_n v_a(t)$$

From Eq. (26), we can see that the dynamic equation includes a conventional stiffness term (the third term) and a nonlinearly coupled cubic stiffness term (the last term), that complicates the frequency response. By dividing Eq. (26) by m_n , the coefficient ($m_n^{-1} k_n$) represents the linear natural frequency. However, the following points should be noted [6]:

1. If the excitation force term is added, peak resonances in natural frequencies may occur.
2. Due to the presence of nonlinear cubic stiffness term, the natural frequency may not be the same as the linear natural frequency and hence nonlinear resonances may occur.
3. The coefficient $m_n^{-1} b_n$ represents the damping term that can enhance vibration suppression of the target dynamic system.
4. There are different methods for modal analysis of nonlinear vibration, however, this topic is beyond the scope of this paper and the reader is referred to [20–22] for more details.

Now let us come back to the problem of vibration control of vibrating beam described in Fig. 2. As abovementioned, the first two mode shapes are considered for control purposes with dynamics described in Eq. (8). It is assumed that dynamic coefficients, nonlinear stiffness and the excitation forcing terms are unavailable and hence adaptive approximation control is selected as a powerful tool for solving the

problem. The control architecture used for vibration suppression is based on Eq. (15a, b) with zero initial conditions for weighting coefficient vectors and amplitudes. The Chebyshev polynomials are used as an approximator with ($\beta = 11$). In effect, increasing the number of terms may not increase the accuracy of tracking/regulation control for the desired references. The key idea of conventional adaptive control is to track the desired reference trajectory with ensured stability while the estimators for uncertainty may not exactly approach to the real value. The control law described in Eq. (15a) consists of a feedforward term and a feedback PD term. The feedback and adaptation gains are listed in Table 1. From Figs. 3 and 4, it is noted that the proposed controller can suppress the vibration of the smart beam very well. In effect, the feedback PD gain plays an important role in tracking and reject disturbances while the feedforward term can reduce the resonance amplitudes within transient regions. The input voltage controls for the two piezo-actuators are shown in Fig. 5. We assumed that the actuators are strong enough that no saturation would occur while in reality, the saturation problem should be considered well for safety.

4 Conclusions

This work deals with adaptive approximation control for regulation of vibration of a flexible beam with piezo-patches considering axial stretching. The axial stretching adds a coupled nonlinear cubic stiffness term and hence the ODE of

the target beam is no longer linear. On the other hand, the AAC is a powerful tool that deals with nonlinearity without need for prior information on the physical parameters of the smart beam and the disturbances if exist. It is a decentralized model-free approach that can cope with different loading and boundary conditions with the same control law. The control law consists of feedforward and feedback terms. The uncertainty is represented by weighting coefficient and orthogonal basis function vectors/matrices. The weighting coefficient matrix is updated with ensured stability based on Lyapunov theory. A simulation of a pinned–pinned beam is performed with two piezo-patches and the results show the verification of the proposed control architecture.

However, future work would be required to investigate the following points:

1. Modelling and nonlinear vibration control of smart beam with large deflection. Large deflection results in a nonlinearly coupled cubic stiffness term that changes the dynamics behaviour of the vibrating beam.
2. Two powerful nonlinear techniques can be proposed to solve the control problem associated with nonlinear large deflection that are approximation based feedback linearization and approximation based backstepping control.
3. The interesting point of the AAC is that it is a model-free technique that can be used for most flexible structures such as vibrating cables, plates and shells. Investigation of the equation of motion for large-scale systems such as plates and shells with large deflection vibration results in ODEs that resemble Eq. (7c) with complex nonlinear terms.

Funding This research received no specific grant from any funding agency in the public, commercial, or not for-profit sectors.

Compliance with ethical standards

Conflict of interest The authors declare that they have no conflict of interest.

References

1. Wagg D, Virgin L (2012) Exploiting nonlinear behavior in structural dynamics. Springer, New York
2. Rao SS (2007) Vibration of continuous systems. Wiley, Amsterdam
3. Chen L-W, Lin C-Y, Wang C-C (2002) Dynamic stability analysis and control of a composite beam with piezoelectric layers. *Compos Struct* 56:97–109
4. Daqaq MF, Alhazza KA, Arafat HN (2008) Nonlinear vibrations of cantilever beams with feedback delays. *Int J Nonlinear Mech* 43:962–978
5. Hosseini SM, Kalhori H, Shooshtari A et al (2014) Analytical solution for nonlinear forced response of a viscoelastic piezoelectric cantilever beam resting on a nonlinear elastic foundation to an external harmonic excitation. *Compos B Eng* 67:464–471
6. Wagg D, Neild S (2010) Nonlinear vibration with control: for flexible and adaptive structures. Springer, Berlin
7. Preumont A (2018) Vibration control of active structures, 4th edn. Springer, Berlin
8. Georgiou G, Foutsitzi GA, Stavroulakis GE (2018) Nonlinear discrete-time multirate adaptive control of non-linear vibrations of smart beams. *J Sound Vib* 423(9):484–519
9. Oveisi A, Gudarzi M (2013) Adaptive sliding mode vibration control of a nonlinear smart beam: a comparison with self-tuning Ziegler–Nichols PID controller. *J Low Freq Noise Vib Active Control* 32:41–62
10. Zhu W-H (2010) Virtual decomposition control: toward hyper degrees of freedom robots. Springer, Berlin
11. Shtessel Y, Edwards C, Fridman L, Levant A (2014) Sliding mode control and observation. Springer, Berlin
12. Slotine J, Li W (1991) Applied nonlinear control. Prentice-Hall, Upper Saddle River
13. Farrell JA, Polycarpou MM (2006) Adaptive approximation based control: unifying neural, fuzzy and traditional adaptive approximation approaches. Wiley, Amsterdam
14. Al-Shuka HFN, Song R (2018) Hybrid regressor and approximation-based adaptive control of piezoelectric flexible beams. In: 2018 2nd IEEE advanced information management, communicates, electronic and automation control conference (IMCEC 2018), pp 330–334
15. Al-Shuka HFN (2017) On local approximation-based adaptive control with applications to robotic manipulators and biped robots. *Int J Dyn Control* 6:1–15
16. Wu J-S (2013) Analytical and numerical methods for vibration analyses. John Wiley & Sons, Singapore
17. Le S (2009) Active vibration control of a flexible beam. MSc. Thesis, San Jose State University
18. Jones DIG (2001) Handbook of viscoelastic vibration damping. Wiley, Amsterdam
19. Wen Yu, Xiaou Li, Irwin GW (2008) Stable anti-swing control for an overhead crane with velocity estimation and fuzzy compensation. R. Lowen and A. Verschoren (eds.), Foundations of generic optimization, volume 2: applications of fuzzy control, genetic algorithms and neural networks, pp 223–240
20. Nayfeh AH, Lacarbonara W, Chin C-M (1999) Nonlinear normal modes of buckled beams: three-to-one and one-to-one internal resonances. *Nonlinear Dyn* 18:253–273
21. Vakakis AF, Manevitch LI, Mikhlin YV, Pilipchuk VN, Zevin AA (1996) Normal modes and localization in nonlinear systems. Wiley, New York
22. Shaw SW, Pierre C (1993) Normal modes for non-linear vibratory systems. *J Sound Vib* 164(1):85–124

Publisher's Note Springer Nature remains neutral with regard to jurisdictional claims in published maps and institutional affiliations.